

SANDIA REPORT

SAND2008-6834

Unlimited Release

Printed October 2008

LDRD Final Report On Synthesis of Shape- and Size-Controlled Platinum and Platinum Alloy Nanostructures on Carbon with Improved Durability

Yujiang Song, John A. Shelnett, Ronald J. Stanis, Robert M. Garcia, and Andres M. Moreno

Prepared by
Sandia National Laboratories
Albuquerque, New Mexico 87185 and Livermore, California 94550

Sandia is a multiprogram laboratory operated by Sandia Corporation,
a Lockheed Martin Company, for the United States Department of Energy's
National Nuclear Security Administration under Contract DE-AC04-94AL85000.

Approved for public release; further dissemination unlimited.

Issued by Sandia National Laboratories, operated for the United States Department of Energy by Sandia Corporation.

NOTICE: This report was prepared as an account of work sponsored by an agency of the United States Government. Neither the United States Government, nor any agency thereof, nor any of their employees, nor any of their contractors, subcontractors, or their employees, make any warranty, express or implied, or assume any legal liability or responsibility for the accuracy, completeness, or usefulness of any information, apparatus, product, or process disclosed, or represent that its use would not infringe privately owned rights. Reference herein to any specific commercial product, process, or service by trade name, trademark, manufacturer, or otherwise, does not necessarily constitute or imply its endorsement, recommendation, or favoring by the United States Government, any agency thereof, or any of their contractors or subcontractors. The views and opinions expressed herein do not necessarily state or reflect those of the United States Government, any agency thereof, or any of their contractors.

Printed in the United States of America. This report has been reproduced directly from the best available copy.

Available to DOE and DOE contractors from

U.S. Department of Energy
Office of Scientific and Technical Information
P.O. Box 62
Oak Ridge, TN 37831

Telephone: (865) 576-8401
Facsimile: (865) 576-5728
E-Mail: reports@adonis.osti.gov
Online ordering: <http://www.osti.gov/bridge>

Available to the public from

U.S. Department of Commerce
National Technical Information Service
5285 Port Royal Rd.
Springfield, VA 22161

Telephone: (800) 553-6847
Facsimile: (703) 605-6900
E-Mail: orders@ntis.fedworld.gov
Online order: <http://www.ntis.gov/help/ordermethods.asp?loc=7-4-0#online>



LDRD Final Report On Synthesis of Shape- and Size-Controlled Platinum and Platinum Alloy Nanostructures on Carbon with Improved Durability

Yujiang Song,¹ John A. Shelnett,¹ Ronald J. Stanis,² Robert M. Garcia,¹ and Andres M. Moreno¹

¹Department of Ceramic Processing and Inorganic Materials 1815

Sandia National Laboratories

P.O. Box 5800

Albuquerque, New Mexico 87185-MS1394

²Fuels and Energy Transitions

Sandia National Laboratories

P.O. Box 5800

Albuquerque, New Mexico 87185-MS0734

Abstract

This project is aimed to gain added durability by supporting ripening-resistant dendritic platinum and/or platinum-based alloy nanostructures on carbon. We have developed a new synthetic approach suitable for directly supporting dendritic nanostructures on VXC-72 carbon black (CB), single-walled carbon nanotubes (SWCNTs), and multi-walled carbon nanotubes (MWCNTs). The key of the synthesis is to creating a unique supporting/confining reaction environment by incorporating carbon within lipid bilayer relying on a hydrophobic-hydrophobic interaction. In order to realize size uniformity control over the supported dendritic nanostructures, a fast photocatalytic seeding method based on tin(IV) porphyrins (SnP) developed at Sandia was applied to the synthesis by using SnP-containing liposomes under tungsten light irradiation. For concept approval, one created dendritic platinum nanostructure supported on CB was fabricated into membrane electrode assemblies (MEAs) for durability examination via potential cycling. It appears that carbon supporting is essentially beneficial to an enhanced durability according to our preliminary results.

ACKNOWLEDGMENTS

This work was supported by the Tier 1 Laboratory Directed Research and Development Program at Sandia National Laboratories. Sandia is a multiprogram laboratory operated by Sandia Corporation, a Lockheed Martin Company, for the United States Department of Energy's National Nuclear Security Administration under Contract DE-AC04-94AL85000.

CONTENTS

1. Introduction.....	7
2. Accomplishments.....	9
3. Conclusions.....	21
4. References.....	23

FIGURES

Figure 1.....	7
Figure 2.....	7
Figure 3.....	9
Figure 4.....	9
Figure 5.....	10
Figure 6.....	11
Figure 7.....	11
Figure 8.....	12
Figure 9.....	12
Figure 10.....	13
Figure 11.....	14
Figure 12.....	15
Figure 13.....	16
Figure 14.....	18

NOMENCLATURE

AA	ascorbic acid
CB	carbon black
CNMs	carbon nanomaterials
CV	cyclic voltammetry
DMFCs	direct methanol fuel cells
DOE	Department of Energy
ECSA	electrochemically active surface area
HAADF	high-angle annular dark-field
MEAs	membrane electrode assemblies
MWCNT	multi-walled carbon nanotube
NHE	normal hydrogen electrode
OCV	open circuit voltage
PEMFCs	proton exchange membrane fuel cells
RDE	rotating disk electrode
RRDE	rotating-ring disk electrode
SNL	Sandia National Laboratories
SnOEP	tin(IV) octaethyl porphyrin
SnP	tin(IV) porphyrin
SWCNT	single-walled carbon nanotube
STEM	scanning transmission electron microscope
TEM	transmission electron microscope

Introduction

Intriguing nanocomposites composed of carbon nanomaterials (CNMs) and supported platinum and platinum alloy nanoparticles have drawn a lot of attention due to their application as electrocatalysts in polymer electrolyte membrane fuel cells (PEMFCs) and direct methanol fuel cells (DMFCs),¹ which have the potential to reduce energy consumption and the nation's dependence on imported petroleum. It is known that carbon supports facilitate the dispersion and stabilization of nanoparticles and reduce nanoparticles aggregation arising from a physical anchoring effect. However, platinum-based nanoparticles supported on CNMs are still subject to sintering and losing surface areas. Previous approaches by alloying platinum nanoparticles with base metals on carbon can only provide electrocatalysts with a lifespan of 2000h before losing up to 50% of the original surface area. How to achieve the targeted 5000h lifespan of electrocatalysts while maintaining or improving their activity set by department of energy (DOE) remains a great challenge.²

As durability and surface area of materials are related to not only the size but the shape of supported platinum and platinum-based alloy, the lack of shape control limits the longevity and broad adoption of these electrocatalysts. Currently, platinum-based electrocatalyst are commonly spherical or semi-spherical. Our proposed solution is to create new bottom-up synthetic methods by combing CNMs and soft templates together to create a special reaction environments and thus directing the nucleation and growth of shape-controlled platinum and platinum alloy

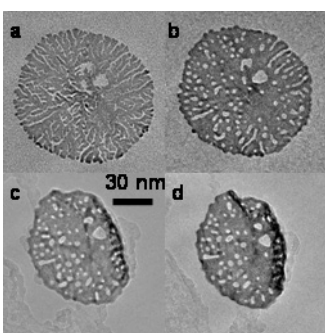


Figure 1. Bright field TEM images showing the structural evolution of a typical flat nanosheet under heating by the electron beam (200 KeV, 500 K) for different time periods: (a) 0, (b) 40, (c) 100 and (d) 110 minutes.

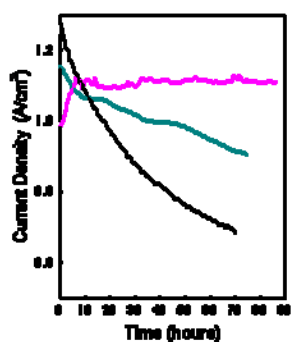


Figure 2. Durability tests of MEAs at 0.5 V for the 7 mg Pt/cm² loadings of dendritic Pt nanospheres (magenta), nanosheets (cyan), and platinum black (black).

electrocatalyst (other than nanoparticles) supported on carbon for durability improvement. We have previously synthesized many free-standing shaped platinum nanostructures, such as dendritic nanosheets (Figure 1a), foam-like nanospheres composed of convoluted dendritic sheets, and nano-wheels by using vesicles,³ aggregated unilamellar liposomes,^{4, 5} and bicelles⁶ as templates, respectively. Interestingly, compared to

unsupported commercial platinum black composed of 5-6 nm nanoparticles, the platinum

nanosheets and foam-like nanospheres exhibited significantly improved durability because of the formation of metastable nanopores evolved from dendritic arms as shown in Figure 1.⁷ Especially, Figure 2 shows that in life tests the fuel cells fabricated with platinum nanosheets and foam-like spheres only exhibited 20% and 0% current density degradation, while the fuel cell made from platinum nanoparticles lost 47% of the original current density.⁷ This encouraging result justified that supporting shaped and ripening-resistant platinum or alloy nanostructures on CNMs to gain added durability is a necessary and reasonable step to take.

In addition, size uniformity control strategy was also proposed for the sake of minimizing Ostwald ripening in which big particles grow into larger ones while small particles shrink until disappear. In contrast to uneven sizes of nanostructures, those with uniform size are inherently resistant to Ostwald ripening. Sandia National Laboratories' (SNL) unique photocatalytic seeding strategy based on a SnP^{3, 5, 8} has been previously demonstrated to be effective for size control over unsupported nanostructures. The mechanism of our photocatalytic seeding is depicted in the following. When a SnP molecule is exposed to visible or ultraviolet light, a photoexcited porphyrin is generated and then reduced by an electron donor like ascorbic acid (AA), forming a porphyrin radical anion that is a strong reducing agent capable of rapidly reducing metal ions from solution. We have used this photocatalytic method to reduce gold, silver, palladium, platinum, and semiconductors. Since the photoreaction is cyclic, each photocatalyst molecule can reduce thousands of metal ions from its surroundings as additional photons are absorbed. Finally, a large number of metal nanoparticles (seeds) are formed in the vicinity of the porphyrin molecules in about 2-3 minutes. The seeding controls the number of nucleation centers and provides each center with a nearly equal growth time, thus producing structures with tunable and uniform sizes. In this project, we aimed to use the photocatalytic seeding to achieve size uniformity control over shaped platinum nanostructures supported on carbon.

Accomplishments

A primary goal of our research is demonstrating the feasibility and effectiveness of our wet-chemical synthetic and photocatalytic seeding technique, and in particular the development of a new synthetic method that produces desired carbon-supported ripening-resistant platinum nanostructures with shapes different from traditional spherical/semi-spherical nanoparticles under solution conditions. We have now successfully designed a unique supporting/confining reaction environment by localizing hydrophobic carbon into hydrophobic lipid bilayer, leading to directed growth of shaped platinum nanostructures on carbon, and approved the concept that carbon supporting can result in added durability after examining MEAs fabricated from the obtained foam-like nanostructures supported on carbon. In addition, we have incorporated commercially available tin(IV) octaethylporphyrin (SnOEP) photocatalysts into lipid bilayer and produced platinum nanoparticles to seed the growth of foam-like platinum nanospheres supported on carbon to realize size uniformity control.

Finally, we have extended the synthesis to generate PtRu and AuPd alloy nanostructures with sheet-like shape potentially beneficial for durability improvement.

Develop wet-chemical synthetic methods needed for confined and supported growth of dendritic platinum nanosheets on carbon. This crucial task—the direct synthesis of dendritic platinum nanostructures on CB—has been accomplished. After extensive screening

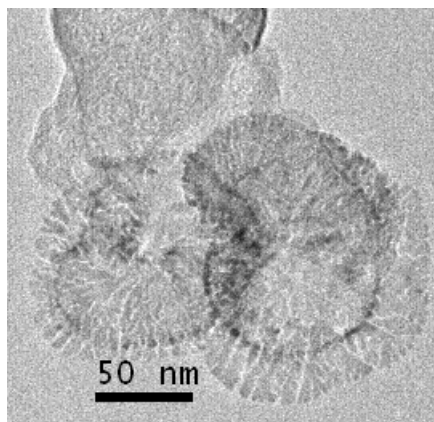


Figure 4. TEM image of dendritic platinum nanosheets supported on VXC-72 CB

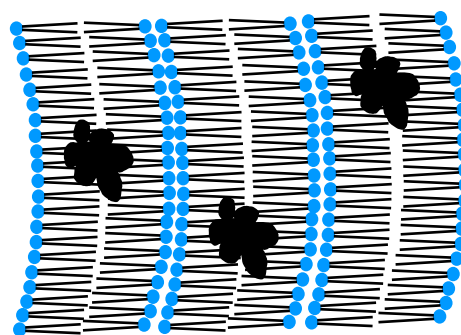


Figure 3. Cartoon of multilayer vesicles containing carbon black, which provide a confined (bilayer) and supported (carbon black) reaction environment

studies, we arrived at the synthetic procedure described briefly here. Initially, multilayer vesicles were prepared by simply mixing DSPC lipids in AA (reducing agent) aqueous solution with the aid of sonication using a water-bath cleaner. A commonly used commercial CB (VXC-72) was added to the vesicle suspension, followed by sonication to well suspend the hydrophobic carbon materials allowing them to be distributed into the hydrophobic region of the lipid layers of vesicles as illustrated in Figure 3. The key of the synthesis is to create a special reaction environment where the growth

of platinum is confined within the liposomal bilayer and simultaneously supported on carbon. An aged aqueous platinum salt⁹ was mixed with the aqueous vesicles containing CB and the mixture was allowed to react under ambient conditions for at least two hours for completion.

Transmission electron microscope (TEM) analysis on the obtained materials revealed the presence of dendritic platinum nanosheets supported on VXC-72 CB as shown in Figure 4. The supported sheets maintain dendritic features suggestive of carrying desired ripening-resistant property. In addition, the introduction of carbon-platinum interaction is expected to bring in a physical anchoring effect likely leading to extra durability improvement. We have mentioned that multilayer vesicles can produce free-standing dendritic platinum nanosheets in the presence of AA and platinum complexes. The confining effect coming from vesicles is crucial for generating dendritic nanostructures. To confirm this point, vesicles in the reaction mixture were left out while holding all the other reaction parameters constant. Consequently, semi-globular platinum nanodendrites were obtained (Figure 5). Unlike the nanosheets with 2-3 nm thickness because of the confining effect, these dendrites obviously take an isotropic growth mode causing the loss of control over the growth along the thickness direction. This result verifies that confined growth did not occur without vesicles involved. On the other hand, it is apparent that CB can well support the platinum growth, since all the platinum nanostructures are associated with

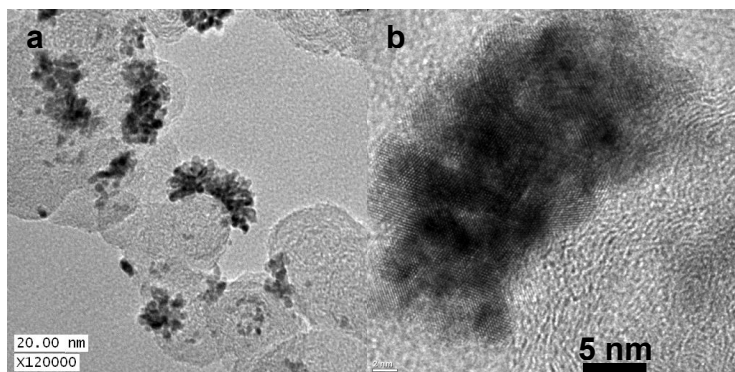


Figure 5. TEM image of semi-globular platinum nanodendrites supported on CB at low (a) and high magnifications (b)

carbon and there are no free platinum present. The synergy arising from the combination of vesicles and CB allows confining and supporting the growth of platinum nanostructures concurrently. However, the problem associated with this synthesis is that some sheets (not shown) seem to possess a small portion of globular dendrite in the center, which is likely an initial nucleation center making the obtained nanostructure deviated from ideal sheets. After extensive studies, this issue remains and more studies are definitely required to optimize the synthesis.

The other free-standing ripening-resistant platinum nanostructures identified previously by us

are foam-like nanospheres composed of interwoven dendritic nanosheets. To support them on carbon is a primary goal, which has been accomplished by using a synthetic strategy similar to that of carbon-supported dendritic platinum sheets. In a typical synthesis, unilamellar liposomes composed of equal moles of DSPC and cholesterol were prepared by a rotary evaporation/incubation/extrusion process in Nanopure water.^{3,4}

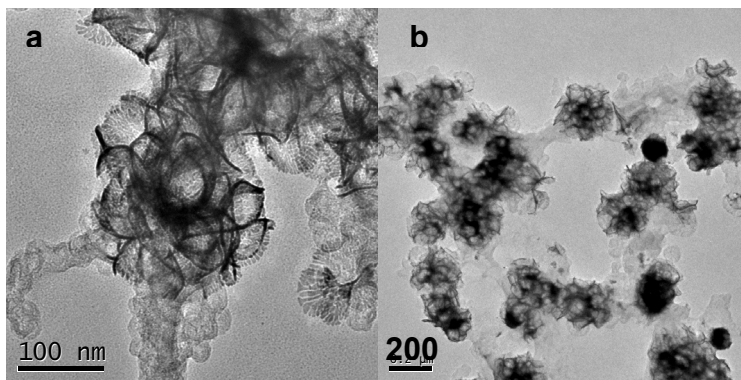


Figure 6. TEM image of foam-like platinum nanospheres supported on carbon black at high (a) and low (b) magnifications

VXC-72 CB was added to the liposomal suspension under sonication to ascertain that hydrophobic carbon has been localized into the hydrophobic region of the lipid bilayer. Finally, solid AA as reducing agent was placed in the reaction vessel and the reaction mixture was allowed to react under ambient conditions for at least two hours. The purpose of adding solid AA is to introduce a significant pH change in the reaction mixture thus inducing unilamellar liposomes to agglomerate together. Previously we have found that the aggregated liposomes as templating agents can lead to the formation of unsupported foam-like platinum nanospheres. TEM analysis (Figure 6) on the resultant materials revealed that foam-like nanospheres supported on carbon were obtained. It is worth pointing out that all the foam-like nanospheres have been supported on carbon, which again confirmed that

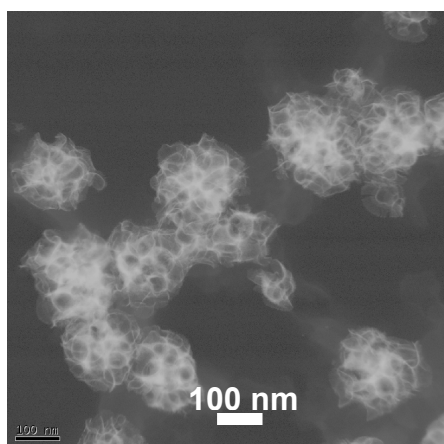


Figure 7. HAADF STEM image of foam-like platinum nanospheres supported on carbon black

hydrophobic carbon is effective for supporting purpose. The dendritic features of the constituent curved sheets are clear in the supported spheres. High-angle annular dark-field (HAADF) scanning TEM (STEM) was also used to characterize the obtained materials. The STEM image as shown in Figure 7 provides an enhanced contrast than regular TEM and allows better examining the interface between platinum and carbon. It appears that the platinum also takes the form of dendritic sheets at the Pt/C interface. However, the supported spheres have a wide size distribution. It is known that during an Ostwald ripening

process big particles grow larger and larger while small ones continuously shrink until disappear. Uneven sizes of particles inherently favor this ripening process. If the size uniformity of the supported spheres can be achieved, it is likely that desired resistance to Ostwald ripening can be added to the foam-like platinum on carbon. To meet this goal, photocatalytic seeding approach recently developed at Sandia is applied to the reaction system as detailed in the following section.

Use photocatalytic seeding to realize size uniformity control over the supported foam-like nanospheres. This is a completed major task. We used the photocatalytic seeding technique to produce platinum nanoparticles (seeds) within liposomal bilayer prior to mixing them up with carbon and other reagents. Hydrophobic SnOEP molecules were placed into liposomal bilayer during the process of preparing liposomes.⁵ The aged platinum complexes were mixed with the SnOEP-containing liposomes suspended in AA aqueous solution. Tungsten light irradiation led to the formation of a large number of nanoparticles (seeds). Figure 8 shows a typical TEM image of obtained platinum seeds organized in circular groups, indicating the templating effect originating from the liposomes which cannot be seen in a TEM image. The liposomes containing seeds were further mixed with CB and extra aged platinum salt for seeded growth of foam-like spheres on carbon. These previously formed

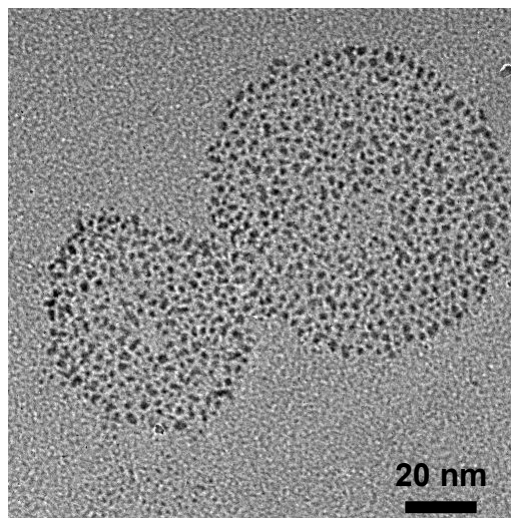


Figure 8. TEM image of platinum nanoparticles (seeds) assembled in circular groups photocatalytically produced by using SnOEP-containing liposomes

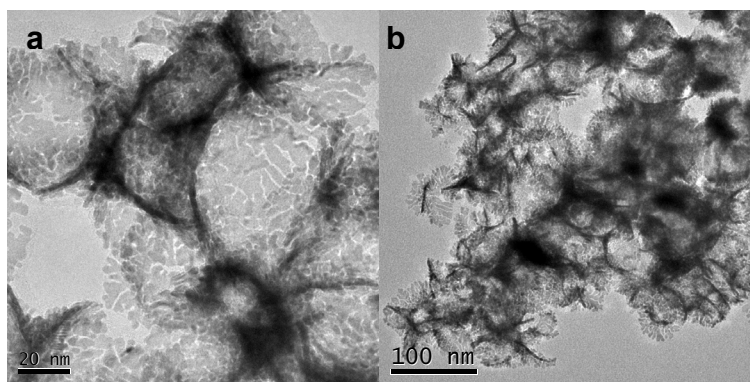


Figure 9. TEM images of seeded foam-like platinum nanospheres supported on carbon at high (a) and low (b) magnifications

nanoparticles can bring a nearly equal growth time for each nucleation center thus offering desired size uniformity. In contrast, in the absence of photocatalytically produced seeds the reaction system experienced a slow and continuous nucleation process³ and the seeds have largely varied growth period causing a wide size distribution.

After attempts, it turned out that our photocatalytic seeding strategy is effective for size uniformity control over the supported nanospheres as shown in Figure 9. The seeded nanostructures are uniform in sizes and smaller in the average diameter than the un-seeded foam-like spheres because of the addition of extra photocatalytically generated seeds. The curved dendritic sheets interweave together but have not reached the spherical shape in that at a constant platinum source there is relatively less amount of platinum distributed to each seed when the total number of seeds increased. This is an essential step toward our ultimate goal of creating ripening-resistant electrocatalysts while retaining or improving the activity. The photocatalytic seeding method is capable of adjusting the number of initial seeds, which means the average sizes of the foam-like spheres on carbon can be tuned by varying the ratio between seeds and metal source. Small foam-like nanospheres are more open than their large version and may be better in terms of mass transportation. In addition, small nanospheres can cover more carbon support, which may be an advantage for the preparation of MEAs.

Support dendritic platinum nanostructures on carbon nanotubes. It is found that single- or multi-walled carbon nanotubes as supports are advantageous over CB as far as durability is concerned.¹⁰ In this regard, we have been successful in extending the synthesis of supported dendritic nanostructures from CB to SWCNTs and MWCNTs. The synthesis procedure with carbon nanotubes involved were the same as for the case of CB described above except that CB was replaced by either SWCNTs or MWCNTs. As shown in Figure 10a, when SWCNTs were utilized in the synthesis, a large percent of the dendritic nanosheets was not supported possibly

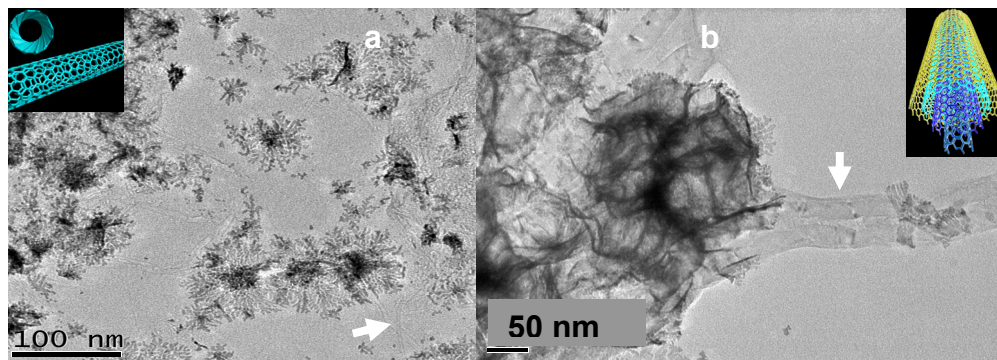


Figure 10. TEM image of dendritic nanosheets on SWCNTs (a) and foam-like nanospheres on MWCNTs (b) with white arrows pointing to carbon nanotubes. (Insets: Illustrations of SWCNTs and MWCNTs.)

because of the relatively small diameter and the high curvature of the SWCNTs, which are not suited to the nucleation and growth of platinum. In

contrast, the MWCNTs are more effective than the SWCNTs for supporting dendritic platinum

nanostructures as shown in Figure 10b. The large sizes of the MWCNTs comparable to those of CB may be the reason why they can well support the platinum nanostructures. This study demonstrated the ability of creating ripening-resistant electrocatalyst supported on different types of carbon materials as long as they are hydrophobic and have a relatively large size. The results further validated our confining/supporting synthetic approach. Reducing the size and manipulating the size uniformity of the spheres supported on MWCNTs by the photocatalytic seeding method might also provide a better metal coating and an increased surface area worthy of future study.

Synthesis of shaped alloy nanostructures with/without carbon support. Since one of our goals is to synthesize ripening-resistant alloy nanostructures and support them on carbon to achieve a better durability, we have investigated the synthesis of a series of alloy nanostructures using unilamellar liposomes as templating agents. This is interesting from the standpoint of determining the applicability of the bilayer templating method for the synthesis of dendritic alloys beyond pure platinum.

This task really has two parts—the first is the creation of

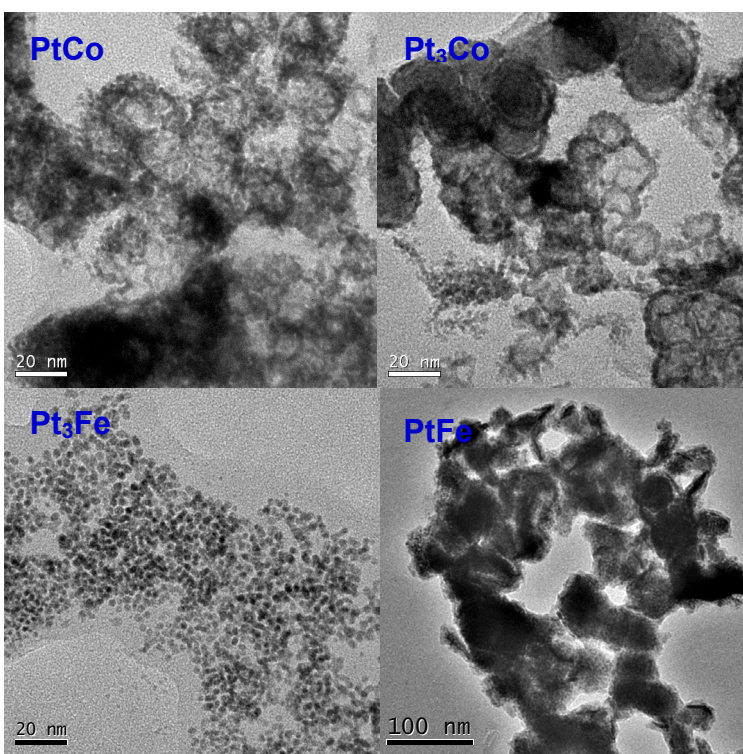


Figure 11. TEM images of platinum-based alloy nanostructures prepared using unilamellar liposomes as templates

various free-standing alloys in the absence of carbon including PtCo, Pt₃Co, PtFe, Pt₃Fe, PtRu, and AuPd. For the synthesis with cobalt, iron or ruthenium complexes involved, we have replaced AA with sodium borohydrides as the reducing agents in that AA is not strong enough to reduce cobalt, iron, or ruthenium complexes. Synthetic procedures used for alloy preparation are the same as those for the free-standing platinum³ except that a mixture of different metal complexes with certain molar ratios was utilized. Briefly, solid sodium borohydride was added to extruded unilamellar liposomes and then mixed with an aqueous solution containing two

different metal complexes with certain molar ratios. The reduction reactions were completed in less than a minute. However, the as-prepared alloys do not have the expected dendritic features based on TEM analysis (Figure 11). For the case of PtCo and Pt₃Co alloy, a mixture of low-

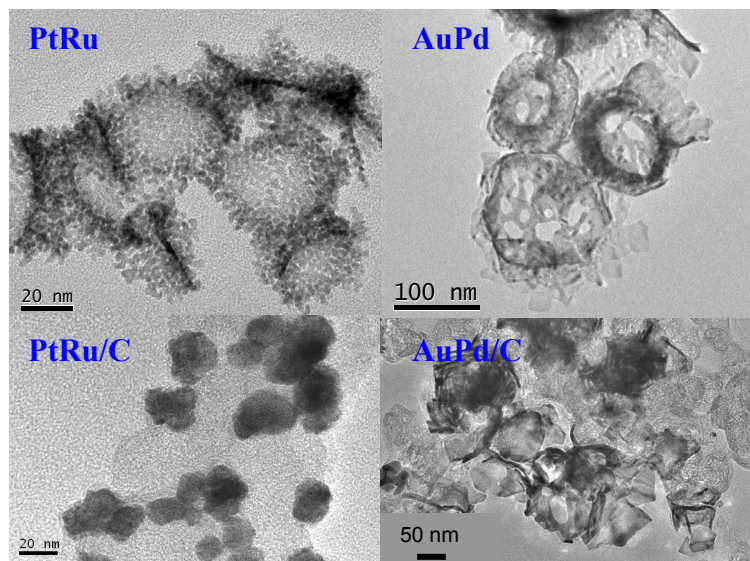


Figure 12. TEM image of PtRu and AuPd alloy nanostructures with/without carbon support

quality hollow nanospheres with irregular nanostructures were obtained. Similarly, Pt₃Fe alloy were in the form of nanoparticles and PtFe alloy ended with irregular shapes. The lack of dendritic shape in the four alloys is possibly related to the employment of sodium borohydrides, which is an extremely strong reducing agent and provides a much faster reducing rate than AA. Another contributor may be a special growth habit of cobalt and iron or their combination with platinum significantly different from platinum. In contrast to these failed trials, we succeeded in the synthesis of PtRu and AuPd alloy by using a similar synthetic approach. Note that in the synthesis of AuPd we used AA as the reducing agent. Figure 12 shows that the PtRu nanostructures are in the form of nearly circular dendritic nanosheets as expected. For the case of AuPd, although the nanostructures do not show dendritic arms, yet they do have sheet-like morphologies with random holes embedded. These two alloy nanostructures offer the opportunity of eventually creating ripening-resistant alloy nanostructures on carbon. The second part of the task is to grow the alloy nanostructures on carbon and image these supported nanostructures using TEM. VXC-72 CB was mixed with the liposomes prior to the addition of reducing agents and metal complexes. The syntheses led to supported alloy nanostructures. As shown in Figure 12, the dendritic PtRu nanosheets became semi-spherical nanoparticles after being supported on carbon. It appears that the confining effect from liposomes did not play a role. It is not clear why this happened. The AuPd nanosheets on carbon retained their original morphology. To summarize, our confining/supporting synthetic strategy is effective in certain scenarios but not universal yet. More investigations are required to gain a better understanding

on how to render our approach more applicable in the synthesis of dendritic alloys with reducing agents other than ascorbic acid.

Structural characterizations of the foam-like nanospheres supported on carbon. Among the electrocatalysts obtained, the foam-like platinum nanospheres on carbon is the best in quality. It is necessary to further characterize the nanospheres for more understanding and future applications in fuel cells. As catalysts, their surface area and electrochemically active surface area (ECSA) are main parameters of interest, because they are directly related to catalytic activity and efficiency. For surface area measurements, the aforementioned synthesis was successfully enlarged to generate sufficient quantities of materials (about 500 mg in a batch) required for macroscopic analysis. The surface area of the spheres was determined to be about 30 m²/g using N₂ adsorption technique. Electrochemical characterizations were conducted in a single-compartment three-electrode cell using a bipotentiostat (Pine Instruments). A rotating-ring disk electrode (RRDE) with a Pt ring (6.25 mm inner-diameter and 7.92 mm outer-diameter) and glassy carbon disk (5.61 mm diameter) was used as the working electrode. The catalyst ink was

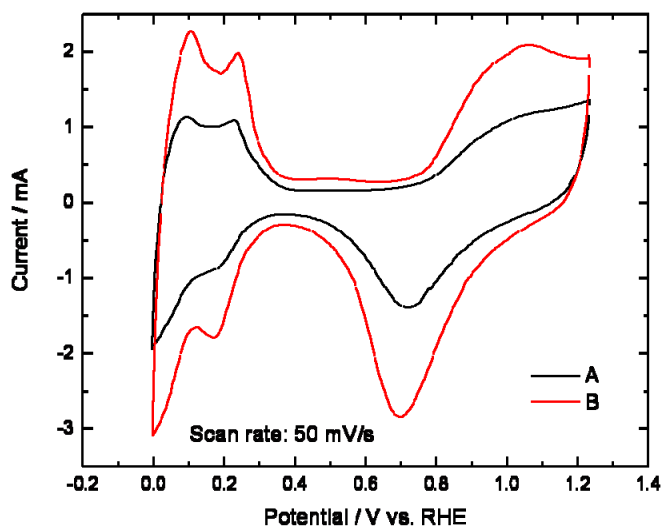


Figure 13. Two repetitions of CV in N₂-saturated 0.5 M H₂SO₄ at scan rate of 50 mV/s

prepared by blending 40 mg of catalyst powder with 4 mL of isopropyl alcohol in an ultrasonic bath. 18.9 μL of the catalyst ink was deposited onto the glassy carbon disk. After drying, 6.3 μL of 0.25 wt % Nafion solution was added on top of the catalyst layer to ensure adhesion of the catalyst on the glassy carbon substrate. A platinum mesh and an Hg/Hg₂SO₄ electrode were used as the counter and reference electrodes, respectively. 0.5 M H₂SO₄ solution was used as the electrolyte. All

potentials in this work were referred to a normal hydrogen electrode (NHE). Initially, the solution was purged with nitrogen and cyclic voltammograms (CVs) were recorded by scanning the disk potential from 1.24 to 0.0 V vs. NHE at a scan rate of 50 mV s⁻¹ as shown in Figure 13. The hydrogen desorption and adsorption peaks were integrated and converted into ECSAs. The ECSA was determined to be 13-21 m²/g using the rotating disk electrode (RDE). For RRDE

measurements, CVs recorded at 5 mV s^{-1} in nitrogen were used to obtain the background capacitive currents. Next, the electrolyte was purged with oxygen for 15 min. The linear sweep voltammograms were recorded at 1200 rpm of the RRDE. The oxygen reduction current was taken as the difference between currents measured in the nitrogen- and oxygen-saturated electrolytes. The mass activity and specific activity of our electrocatalysts determined by RRDE are 5.6-6.3 A/g_{Pt} and 35-42 $\mu\text{A/cm}^2_{\text{Pt}}$ at 0.85 V, respectively. The mass and specific activity of commonly used commercial ETEK electrocatalyst Pt/C determined under the same conditions is 3.2 A/g_{Pt} and 35 $\mu\text{A/cm}^2_{\text{Pt}}$ at 0.85 V, respectively. In summary, our electrocatalyst is similar to the commercial one in terms of mass and specific activity. These results verify that our electrocatalysts basically retain the activity while may potentially improve durability. In other words, durability enhancement, if exists, will not sacrifice the activity of catalysts.

Durability examination by potential cycling. An important topic remained to be addressed is if the supported foam-like spheres have an improved durability than the un-supported ones. In order to answer this question, the supported nanospheres were fabricated into MEAs. Briefly, catalyst coated gas diffusion electrodes were prepared by spray-coating catalyst ink slurry onto the microporous layer of 35BC paper electrodes (SGL carbon). The geometric surface area was 10cm^2 . Spraying was done using a custom designed computer controlled X-Y system and using a syringe pump for controlled ink delivery. Anodes used in the experiment had a catalyst loading of 0.4mg Pt/cm^2 (20% Pt on Vulcan XC72, E-tek) containing 25wt% Nafion. Cathodes used had catalyst loadings of 0.4mg Pt/cm^2 using the catalyst of interest and 25wt% Nafion. Nafion 212 was purchased from Ion Power and was pretreated by boiling for 1 hour each in solutions of 3% H_2O_2 , DI water, 1M H_2SO_4 and DI water. After pretreatment the Nafion 212 was stored in DI water in a sealed container in the dark. MEAs were prepared by hot pressing at 145°C and 2000lbs of force for 6 minutes for Nafion MEAs. For comparison, MEAs comprising of free-standing foam-like nanospheres were also prepared using the same procedure. MEAs with electrode geometric surface areas of 10cm^2 were assembled into fuel cell hardware (Fuel Cell Technologies) and tested using Fuel Cell Technologies test stations. The load control, gas flows, humidifier temperatures, cell temperature, and backpressure were all controlled by the test stations. During testing the cell hardware was controlled at 80°C , gas flow rates of 400 sccm were used, and backpressure of 30psig was maintained. The inlet gases were fed through humidifiers were controlled at 80°C . UHP H_2 , and industrial grade oxygen were used for fuel cell

performance evaluation. Polarization curves were measured by scanning the voltage from open circuit voltage (OCV) to 0.7V with a step size of 0.01V holding each step for 6 minutes before the data point is recorded. Below 0.7V a step size of 0.05V was used down to 0.25V at which load was removed. Potential cycling experiments were done by feeding H₂ to the anode electrode and UHP N₂ to the cathode electrode. The potential was then cycled between 1.1 and 0.6V vs. RHE at a scan rate of 20mV/s.

An eight day protocol was used to evaluate the fuel cell performance and catalyst durability. On day one initial polarization curves were measured, and a 24 hour break in protocol of alternating half hour constant voltage holds of 0.5 and 0.6V (under H₂/O₂) was

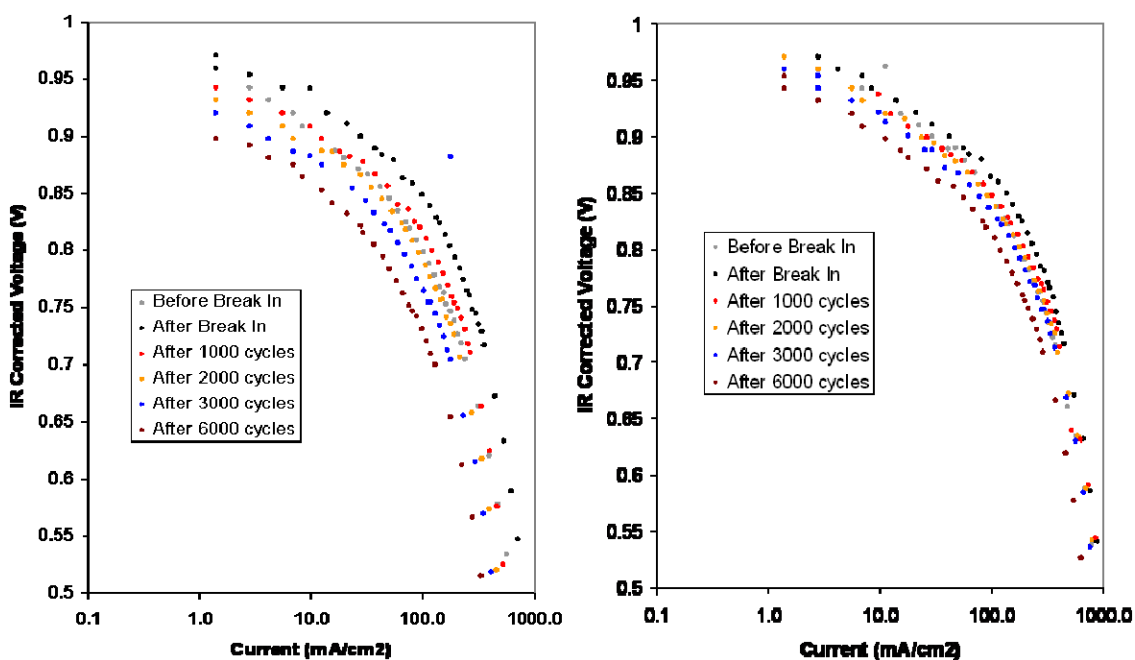


Figure 14. Polarization curves of MEAs fabricated from unsupported (a) and supported (b) foam-like nanospheres during a break in and following potential cycling process.

begun. On day two, once the break-in was complete, polarization curves were measured and a series of 1000 potential cycles was begun which ran overnight. On day three the polarization curves were measured and an additional 1000 cycles were started. On day four through seven the same measurements were repeated. By the start of day eight the MEA had experienced 6000 potential cycles, at this point polarization curves were measured again and then the test was ended.

Figure 14 shows that the MEAs apparently experienced performance enhancement after break in and decayed during the following potential cycling process in terms of current density. The

potential cycling (0.6-1.1 V) accelerates the aging of electrocatalyst and represents much severer conditions for durability test than holding a cell potential at 0.5 V, in which for the MEA made of the free-standing nanospheres no degradation was observed during a 75-h FC test as described previously. It is worth pointing out that the degradation degree of the supported spheres is much less than that of the unsupported spheres. For example, at 0.71 V the MEAs made of supported and unsupported spheres lost 37.4% and 68% of their respective original current density after 6000 cycles. This result verifies that our ultimate goal of gaining added durability by carbon supporting was achieved. However, we have realized that the FC test data and electrochemical measurements are preliminary and more repetitions are needed for validation. Especially, a new MEA fabrication method suitable for our new electrocatalysts should be developed for exploring more advantages of our electrocatalysts, such as a better mass transportation due to the openness of the foam-like nanospheres. In addition, the three-phase boundary (porous carbon/Pt/Nafion) is definitely required to be manipulated to ensure each nanosphere has electron and proton pathway as well as porous channels accessible for gas diffusion and water removal. Insert text here.

Conclusion

Platinum-based electrocatalysts are the key components in proton exchange membrane fuel cells (PEMFC) to catalyze hydrogen oxidation and oxygen reduction at anode and cathode, respectively. During the catalytic process, the electrocatalysts generally in the form of spherical/semi-spherical nanoparticles are prone to ripen and lose their activity. The low durability of electrocatalysts is a technological barrier and impedes the commercialization of PEMFC. To overcome the durability issue of the electrocatalysts, carbon supporting and alloying with base metals have been widely employed. However, these approaches can only lead to an electrocatalyst with 2000h of lifespan. How to meet the 5000h of lifespan by 2010 announced by DOE remains a challenge. Recently, we discovered that free-standing dendritic platinum nanostructures created at Sandia have improved durability compared with commercial platinum black composed of unsupported semi-spherical nanoparticles. The durability enhancement originates from unique dendritic shape of our platinum nanostructures different from spherical/semi-spherical nanoparticles. In this project, we aimed to gain added durability by supporting dendritic platinum nanostructures on carbon and/or alloying them with base metals. For this purpose, we have developed a new synthetic approach suitable for directly supporting the dendritic nanostructures on a variety of carbon nanomaterials including VXC-72 carbon black (CB), single-walled carbon nanotubes (SWCNTs), and multi-walled carbon nanotubes (MWCNTs). The key of the synthesis is to creating a unique supporting/confining reaction environment by incorporating carbon into lipid bilayer relying on a hydrophobic-hydrophobic interaction. Dendritic platinum nanosheets and foam-like platinum nanospheres composed of convoluted sheets were successfully supported on carbon. We have also extended the synthesis to unsupported dendritic PtRu and AuPd nanosheets. In particular, the AuPd alloy nanosheets were supported on CB. In order to realize size uniformity control over the supported foam-like spheres, a fast photocatalytic seeding method based on tin(IV) porphyrins (SnP) developed at Sandia was applied to the synthesis by using SnP-containing liposomes under tungsten light irradiation. For concept approval, the foam-like platinum nanospheres on CB were selected among the obtained nanomaterials and fabricated into membrane electrode assemblies (MEAs) for durability examination via potential cycling. It appears that carbon supporting is essentially beneficial to a better durability according to our preliminary results. Since our dendritic platinum nanostructures with/without carbon supports represent a new class of electrocatalysts,

appropriate MEA fabrication method and FC test conditions correspondingly need to be developed to more accurately quantify the durability improvement and other FC performance parameters of our electrocatalysts.

References

- (1) Vielstich, W.; Lamm, A.; Gasteiger, H. A. (Eds.), *Handbook of Fuel Cells - Fundamentals, Technology and Applications* John Wiley & Sons: New York, **2003**.
- (2) *Department of Energy-Multi-Year Research and Development Plan-3.4 Fuel Cells: Table 3.4.12 Electrocatalyst Targets for Transportation Applications, 2007*, <http://www.eere.energy.gov/hydrogenandfuelcells/mypp/>, Vol. 3.4-24.
- (3) Song, Y. J.; Yang, Y.; Medforth, C. J.; Pereira, E.; Singh, A. K.; Xu, H. F.; Jiang, Y. B.; Brinker, C. J.; Swol, F. v.; Shelnut, J. A. *J. Am. Chem. Soc.* **2004**, *126*, 635-645.
- (4) Song, Y. J.; Steen, W. A.; Pena, D.; Jiang, Y. B.; Medforth, C. J.; Huo, Q. S.; Pincus, J. L.; Qiu, Y.; Sasaki, D. Y.; Miller, J. E.; Shelnut, J. A. *Chem. Mater.* **2006**, *18*, 2335-2346.
- (5) Song, Y. J.; Garcia, R. M.; Dorin, R. M.; Wang, H. J.; Qiu, Y.; Shelnut, J. A. *Angew. Chem. Int. Ed.* **2006**, *45*, 8126-8130.
- (6) Song, Y. J.; Dorin, R. M.; Garcia, R. M.; Jiang, Y. B.; Wang, H. R.; Li, P.; Qiu, Y.; van Swol, F.; Miller, J. E.; Shelnut, J. A. *J. Am. Chem. Soc.* **2008**, *in press*.
- (7) Song, Y. J.; Hickner, M. A.; Dorin, R. M.; Garcia, R. M.; Wang, H. R.; Jiang, Y. B.; Qiu, Y.; Challa, S. R.; van Swol, F.; Medforth, C. J.; Miller, J. E.; Nwoga, T.; Kawahara, K.; Li, W.; Shelnut, J. A. **2008**, *in preparation*.
- (8) Song, Y. J.; Jiang, Y. B.; Wang, H. R.; Pena, D. A.; Qiu, Y.; Miller, J. E.; Shelnut, J. A. *Nanotechnology* **2006**, *17*, 1300-1308.
- (9) Ciacchi, L. C.; Pompe, W.; De Vita, A. *J. Am. Chem. Soc.* **2001**, *123*, 7371-7380.
- (10) Wang, J. J.; Yin, G. P.; Shao, Y. Y.; Wang, Z. B.; Gao, Y. Z. *J. Phys. Chem. B* **2008**, *112*, 5784-5789.

DISTRIBUTION

1	MS1349	Bill Hammetter	1815
10	MS1349	Yujiang Song	1815
2	MS9018	Central Technical Files	8944
2	MS0899	Technical Library	4536
1	MS0123	D. Chavez, LDRD Office	1011